



## Effect of sulphuric acid pretreatment concentration on the behaviour of $\text{CoO}_x/\gamma\text{-Al}_2\text{O}_3\text{-SO}_4$ monolithic catalysts in the lean $\text{CH}_4\text{-SCR}$ process

J.C. Martín <sup>a</sup>, S.B. Rasmussen <sup>a,\*</sup>, S. Suárez <sup>b</sup>, M. Yates <sup>a</sup>, F.J. Gil-Llambías <sup>c</sup>, M. Villarroel <sup>c</sup>, P. Ávila <sup>a</sup>

<sup>a</sup> Instituto de Catálisis y Petroleoquímica, CSIC, Calle Marie Curie 2, Cantoblanco, 28049 Madrid, Spain

<sup>b</sup> CIEMAT-PSA, Environmental Applications of Solar Radiation Unit, Avda. Complutense 22, Building 42, Madrid, Spain

<sup>c</sup> Facultad de Química y Biología, USACH, Casilla 40, Correo 33, Santiago, Chile

### ARTICLE INFO

#### Article history:

Received 17 March 2009

Received in revised form 8 June 2009

Accepted 12 June 2009

Available online 21 June 2009

#### Keywords:

$\text{CH}_4$

SCR

Monolith

$\text{DeNO}_x$

Cobalt

Alumina

UV-vis

Zeta potential

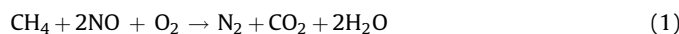
### ABSTRACT

The pretreatment of conformed  $\gamma$ -alumina monolithic supports with sulphuric acid solutions induces an increase in the activity of  $\text{CoO}_x/\gamma\text{-Al}_2\text{O}_3$  catalysts for the selective catalytic reduction of nitrogen oxides employing methane as the reductant. The improvement in the activity was related to the acid strength of the acid used in the pretreatment step, where both the activities and selectivities were found to be greatest when the monolithic supports were pretreated with a 2.5 M  $\text{H}_2\text{SO}_4$  solution. The UV-vis-NIR, XRD spectroscopies, zero point charge measurements and TGA studies demonstrated that the active cobalt phase was stabilised as a tetrahedral Co(II) complex, possibly associated to sulphate ligands. UV-vis-NIR spectroscopy further revealed that pretreatment with 2.5 M  $\text{H}_2\text{SO}_4$  led to the lowest ratios of crystalline  $\text{Co}_3\text{O}_4$ , explaining the enhanced activity and higher selectivity, since this compound is known to promote the undesirable direct methane combustion with oxygen. Furthermore, TGA analysis combined with zeta-potential measurements, lead to the conclusion that the acidity, important for the activation of methane, increased on the catalyst surface with increasing acid concentration up to 2.5 M  $\text{H}_2\text{SO}_4$ , whereafter formation of  $\text{Al}_2(\text{SO}_4)_3$  took place, that lowered the catalytic activity due to the formation of non-selective cobalt oxide clusters.

© 2009 Elsevier B.V. All rights reserved.

## 1. Introduction

The catalytic reduction of  $\text{NO}_x$  with hydrocarbons under lean conditions may be used for the abatement of  $\text{NO}_x$  contamination from both mobile and stationary sources [1–6]. The use of methane as the reductant is especially attractive due to its availability as the primary component in natural gas, easy handling characteristics and low cost [7]. The proposed stoichiometry of the  $\text{CH}_4\text{-SCR}$   $\text{DeNO}_x$  reaction is the following:



However, methane is not easily activated, which results in relatively low turnover frequencies for the reaction in Eq. (1), compared with other hydrocarbons such as propene [8]. Development of catalysts based on cobalt (II) supported on MFI-zeolites [9,10] or sulphated zirconias [11,12] have provided advancements and promise for the possible viability of methane based SCR. A recent *operando* study on a Co-H-MFI catalyst indicated that  $\text{Co}^{3+}$  could be the active cobalt species, able to convert NO to adsorbed higher oxidation states  $\text{N}_x\text{O}_y$ , possibly as bridging nitrates species

[13]. In that work it was suggested that the active site could be located within the cavities of the zeolite either as isolated  $\text{Co}^{3+}$  or small cobalt oxide clusters. Recently from IR spectroscopy studies of  $\text{CoO}_x/\text{MOR}$  it was reported that isolated  $\text{Co}^{3+}$  appeared to be the active species for the  $\text{DeNO}_x$  reaction [14]. Furthermore, it has been suggested that the function of the  $[\text{Co}-\text{O}-\text{Co}]^{2+}$  moieties present at higher loadings were at most only spectator species, concluding that the structure of the active isolated  $\text{Co}^{2+}$  site for NO abatement with  $\text{CH}_4$  in lean conditions remained to be identified [15]. For  $\text{Co}/\gamma\text{-Al}_2\text{O}_3$  based catalysts it has been claimed that isolated  $\text{Co}^{2+}$  was the active site and thus dispersion of cobalt was important in order to avoid formation of the  $\text{Co}_3\text{O}_4$  spinel crystalline structure that promotes the undesirable methane combustion reaction [16].

Previously, we have shown for the  $\text{Co}/\gamma\text{-Al}_2\text{O}_3$  system that the pretreatment of monolithic alumina with sulphuric acid led to higher activities and selectivities compared to samples treated with other mineral acids such as hydrochloric, nitric or phosphoric [17]. The higher activity and selectivity was related to the stability of Co(II) species and the presence of surface sulphate species. Furthermore, recent results on acid treated  $\text{Co}/\gamma\text{-Al}_2\text{O}_3\text{-SO}_4$  catalysts conformed as monolithic structures indicated that the catalysts maintained around 40% of its original activity in the presence of water vapour, which could be related to slow water

\* Corresponding author. Tel.: +34 915854873; fax: +34 945854760.

E-mail address: [sbrasmussen@icp.csic.es](mailto:sbrasmussen@icp.csic.es) (S.B. Rasmussen).

diffusion compared to CH<sub>4</sub> and NO in the porous monolithic structures [18]. In this study, the influence of the alumina sulphidation on catalytic activity, selectivity as well as textural properties and the role of sulphate species in the stabilisation of cobalt species has been analysed on catalysts conformed as open channel monolithic supports, comparing samples pretreated with solutions of different concentrations of H<sub>2</sub>SO<sub>4</sub>. Sulphidation of conformed materials is complicated since both the macroporosities and mechanical strengths should be considered when evaluating the best candidates eligible for use at industrial scale. The acid treatment was carried out by immersion of the calcined alumina monoliths in acidic solutions of known strength for a fixed period of time. This method was chosen since it normally yields controlled depositions, with optimised dispersion and minimal damage to the conformed support structures.

## 2. Experimental

### 2.1. Catalyst preparation

The alumina monolithic support was prepared by extrusion of a commercial boehmite, Pural SB (Condea/Sasol) that had previously been formed into a paste with adequate rheological properties by the addition of temporary additives such as organic binders and lubricants. The honeycomb structured supports were dried at ambient temperature, then at 110 °C and finally calcined at 500 °C for 4 h. The resulting monoliths had 49 channels (7 × 7), a square channel size of 2.0 mm and a wall thickness of 1.1 mm to give a cell density of 10.7 cells/cm<sup>2</sup> and geometric area of 847 m<sup>2</sup>/m<sup>3</sup>. Pretreatment of the alumina support with H<sub>2</sub>SO<sub>4</sub> solutions of different concentrations (1.0, 1.8, 2.5 and 3.2 mol l<sup>-1</sup>) was done by immersion of the monoliths into the chosen solution for 30 min. Subsequently the monoliths were withdrawn, excess solution allowed to drain and then dried at 110 °C and re-calcined at 500 °C for 4 h. The active phase was incorporated on to pieces of monolithic support of 10 cm length by immersion into an aqueous solution (0.56 M) of cobalt(II) nitrate hexahydrate (Co(N-O<sub>3</sub>)<sub>2</sub>·6H<sub>2</sub>O) (A.C.S. Sigma-Aldrich) at a pH of around 5.8, followed by subsequent drying and calcination as described above.

### 2.2. Catalytic activity

The catalytic activities were determined in a continuous flow tubular reactor operating in an integral regime at close to isothermal conditions using an 85 cm stainless steel reactor with an internal diameter of 3.5 cm. The free space between the monolithic catalyst and the reactor wall was filled with inert alumina wool, to guarantee that the gas feed passed through the monolith channels. The operating conditions were: [NO] = 500 ppm, [CH<sub>4</sub>] = 1000 ppm, [O<sub>2</sub>] = 5 vol.%, balanced in N<sub>2</sub>, temperature = 350–575 °C, P = 120 kPa, GHSV(N.T.P.) = 5120 h<sup>-1</sup>, ν<sub>L</sub>(N.T.P.) = 0.39 m s<sup>-1</sup> and total flow F(N.T.P.) = 3500 ml min<sup>-1</sup>. The NO, NO<sub>x</sub> and NO<sub>2</sub> concentrations at inlet and outlet were continuously measured by chemiluminescence with a Signal Series 4000VM NO<sub>x</sub> analyser. The CH<sub>4</sub> was analysed using a flame ionisation detector, Horiba THC-FIA-510, while the CO<sub>2</sub> concen-

tration at the reactor outlet was monitored by infrared spectroscopy using a Horiba VIA-510 analyser.

### 2.3. Catalyst characterisation

Crystalline phases were determined by X-ray diffraction (XRD) on powdered samples with a Seifert 3000P diffractometer with a nickel filter using a Cu K<sub>α1</sub> radiation with a wavelength of  $\lambda = 1.5406$  nm. The spectra were measured over the  $2\Theta = 10$ –80° range with a 0.02° step with a 2 s/step acquisition rate. Identification of the crystalline species was made using the RAYFLEX-Analyze 2.25 software.

The crushing strengths of the monoliths were determined using a Chatillon LTCM dynamometer with a 0.73 mm diameter test head, 10 measurements were made on each sample to ensure the precision of the result.

The cobalt species in the catalysts were analysed by UV/vis spectroscopy. The spectra were recorded on dry samples using a Varian Cary 5000 UV-vis spectrophotometer. The measurements were made with a spectral bandwidth of 5 nm, in the 250 to 2500 nm range. The signal averaging times were 1 s, in 'double beam' mode, using full slit height and baseline corrections.

The cobalt contents were determined by X-ray fluorescence (XRF) using a Seifert EXTRA-II spectrometer, equipped with two fine focus X-ray lines, Mo and W anodes a Si(Li) detector with an active area of 80 mm<sup>2</sup> and a resolution of 157 eV at 5.9 keV (Mn K<sub>α</sub>).

The zero point charge (ZPC) of the support materials before cobalt impregnation was determined by measuring the zeta potential as a function of the solution pH. The zeta potentials were obtained using the Helmholtz-Smoluchowski equation:  $\bar{V} = 1/4\epsilon\zeta/\pi\eta$ , measuring the electrophoretic migration rate in a Zeta-Meter Inc. Instrument model 3.0+, provided with an automatic sample transfer unit (peristaltic pump and special electric pinch clamp) to avoid sample sedimentation problems [15]. In this equation  $\bar{V}$  is the electrophoretic mobility,  $\epsilon$  the permittivity,  $\zeta$  the zeta potential and  $\eta$  the dynamic viscosity. Experiments were carried out using 30 mg of <2 μm powder samples suspended in 200 ml of 10<sup>-3</sup> M KCl, adjusting the pH with 0.2 M KOH and HCl solutions. Not more than one type of particle was detected in any sample, with each curve recorded at least twice to ensure the reproducibility of the results.

The thermal gravimetric analyses of the samples were carried out on a Netzsch 409 EP simultaneous thermal analysis device. The TGA-DSC curves were measured using approximately 20–30 mg of powdered sample which were heated in an air flow of 75 ml min<sup>-1</sup> at a rate of 5 °C min<sup>-1</sup> from room temperature to 1000 °C, using α-alumina as reference. Sulphate contents were determined by considering the difference in weight loss between each sulphated sample and the non-sulphated one, assuming the sulphate decomposition reaction as: M-SO<sub>4</sub> → M-O + SO<sub>2</sub> + 1/2O<sub>2</sub>.

## 3. Results and discussion

The main characteristics of the synthesised samples are shown in Table 1. Due to their similarities reasonably constant cobalt contents between 3 and 4% were obtained. From the cobalt

**Table 1**

Textural properties and cobalt content of the synthesised catalyst samples.

Catalyst	[H <sub>2</sub> SO <sub>4</sub> ] (mol l <sup>-1</sup> )	Total pore volume <sup>a</sup> (cm <sup>3</sup> g <sup>-1</sup> )	Surface area (S <sub>BET</sub> ) (m <sup>2</sup> g <sup>-1</sup> )	Co XRF (% wt)	S TGA (% wt)	Mechanical strength (kg cm <sup>-2</sup> )
CoAl	–	0.80	220	4.0	0.0	215
CoAlS1.0	1.0	0.82	201	3.1	3.0	203
CoAlS1.8	1.8	0.78	202	3.0	4.7	190
CoAlS2.5	2.5	0.73	192	3.0	5.0	191
CoAlS3.2	3.2	0.88	199	3.4	5.9	161

<sup>a</sup> Total pore volume (for the pore diameter range 0–10 μm) calculated by combining results from MIP and N<sub>2</sub>-physisorption measurements.

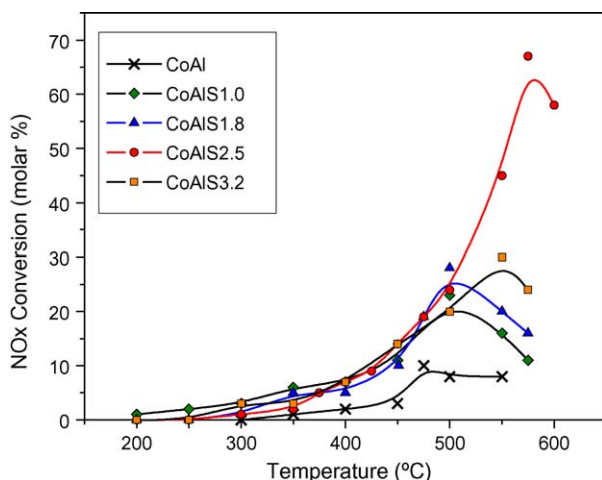


**Fig. 1.** H<sub>2</sub>SO<sub>4</sub> concentration effect on the catalytic activity of CoO<sub>x</sub>/Al<sub>2</sub>O<sub>3</sub>-SO<sub>4</sub> catalysts series for NO reduction.

contents determined by XRF it may be appreciated that the values were quite similar for all except the untreated support. The difference in this latter case probably arises from the relative higher amount of available anchoring sites on a non-sulphated surface.

The specific surface areas ( $S_{\text{BET}}$ ) for the sulphated samples were all around 200 m<sup>2</sup> g<sup>-1</sup> with no significant tendencies, while the un-sulphated sample exhibited a slightly higher area, 220 m<sup>2</sup> g<sup>-1</sup>. The mechanical strengths were generally observed to decrease slightly with increasing H<sub>2</sub>SO<sub>4</sub> solution concentration.

In Fig. 1 the NO conversions of the sulphated catalysts are plotted as a function of temperature. The un-sulphated sample exhibited very poor NO-SCR activity, whereas the activities of the sulphated samples increased in a similar steady Arrhenius like fashion for all samples up to 500 °C. Thereafter each sample reached a maximum conversion value, with the tendency that CoAlS2.5 > CoAlS3.2 > CoAlS1.8 > CoAlS1.0 > CoAl. The maximum conversion temperatures of the catalysts were directly related to their methane combustion activities with the oxygen present in the gas mixture. The methane oxidation results under these operating conditions in the presence of NO are shown in Fig. 2.

Comparing Figs. 1 and 2, a number of observations can be drawn. The apparent activation energies of the sulphated catalysts for NO reduction at low temperature ( $T < 450$  °C) were all similar, with values close to 62.3 kJ mol<sup>-1</sup>. The

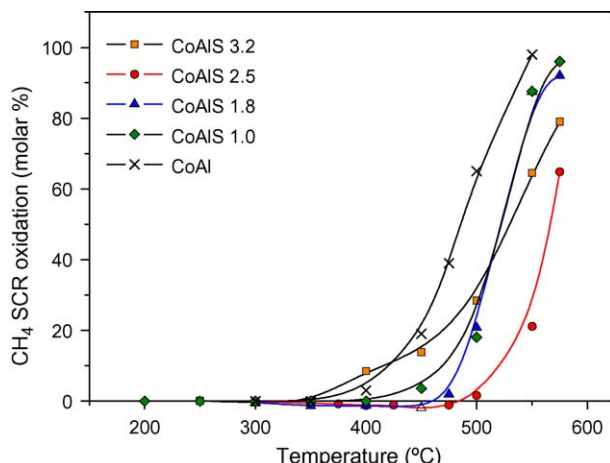


**Fig. 2.** H<sub>2</sub>SO<sub>4</sub> concentration effect on the catalytic activity of CoO<sub>x</sub>/Al<sub>2</sub>O<sub>3</sub>-SO<sub>4</sub> catalysts series for the CH<sub>4</sub> oxidation in the presence of NO.

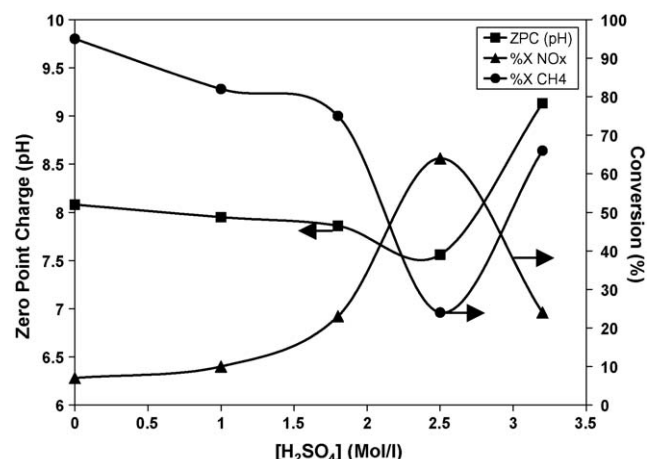


**Fig. 3.** Influence of the H<sub>2</sub>SO<sub>4</sub> concentration on the zero point charge of the catalysts and on the catalytic activity for NO<sub>x</sub> reduction and CH<sub>4</sub> oxidation at 550 °C.

differences between the behaviour of these catalysts at higher temperatures were related to the extension of the competitive CH<sub>4</sub> oxidation reaction, such that maximum NO conversion coincided with the temperature at which 50% methane oxidation occurred. These results indicate that the active sites for NO reduction are present in all sulphated catalyst samples and their different behaviours in the overall process were due to differences in the sites responsible for the direct CH<sub>4</sub> combustion with oxygen, with the un-sulphated CoAl sample exhibiting the highest CH<sub>4</sub> combustion activity.

In order to further clarify and explain the behaviour of this catalyst series zero point charge/isolectric point measurements were carried out. The ZPC tendency with increasing acid concentration is presented in Fig. 3 along with the variation of the values of the NO<sub>x</sub> reduction obtained with these catalysts at 550 °C.

The activities of the NO<sub>x</sub> reduction of the catalysts increase steadily with increasing sulphate concentration up to the impregnation solution of 2.5 M H<sub>2</sub>SO<sub>4</sub>. However, the NO<sub>x</sub> reduction value was markedly lower for the catalyst prepared with the 3.2 M solution. For the competitive reaction of CH<sub>4</sub> oxidation the opposite behaviour was observed. Here the activities decreased with the increasing sulphate concentration up to the value of 2.5 M of H<sub>2</sub>SO<sub>4</sub>, then rose steeply for the catalyst pretreated with the 3.2 M solution.

Comparing the variation of the ZPC of these materials and the CH<sub>4</sub> oxidation activity, a clear relationship was observed. An increased surface acidity was seen after pretreatment with H<sub>2</sub>SO<sub>4</sub> between 0 and 2.5 M due to the incorporation of higher amounts of H<sup>+</sup> on the surface. However, above 2.5 M a dramatic increase in ZPC was observed, which correlated well with the formation of a new Al<sub>2</sub>(SO<sub>4</sub>)<sub>3</sub> phase in accordance with the XRD measurements presented in Fig. 4. In terms of DeNO<sub>x</sub> activity, the most active catalyst formulation was synthesised from the 2.5 M H<sub>2</sub>SO<sub>4</sub> sulphating solution. This support had a ZPC value of 7.8, and constituted the minima within the sample array tested, as seen in Fig. 3. This corresponded to a maximum in the selectivity of NO<sub>x</sub> reduction versus CH<sub>4</sub> oxidation which was related with the formation of Co spinel on the catalyst surface [17].

The powder XRD plots in Fig. 4 compares the sulphated supports with the untreated sample. It appears that increasing the concentration of H<sub>2</sub>SO<sub>4</sub> up to 2.5 M did not alter the diffractograms significantly, though it could appear that increasing concentration yielded decreased crystallinity of the γ-Al<sub>2</sub>O<sub>3</sub>. At the maximum concentration (3.2 M) new peaks appeared that could be assigned to the formation of Al<sub>2</sub>(SO<sub>4</sub>)<sub>3</sub>.

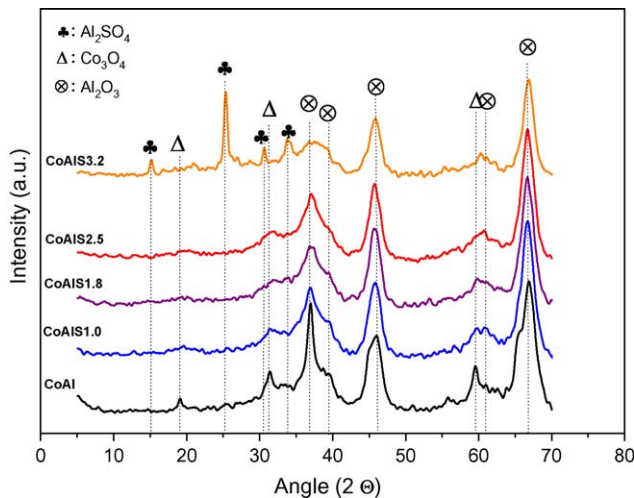


Fig. 4. X-ray diffraction for  $\text{CoO}_x/\text{Al}_2\text{O}_3\text{-SO}_4$  catalysts.

The un-sulphated sample exhibited characteristic peaks for the cobalt spinel crystal structure  $\text{Co}_3\text{O}_4$ , which subsequently disappeared with increasing concentration of  $\text{H}_2\text{SO}_4$  in the solution. Although the existence of cobalt spinel for the CoAlS3.2 could not be verified by XRD, its presence was detected by UV-vis spectrometry, shown in Fig. 5. This apparent discrepancy is probably related to different nucleation mechanisms for  $\text{Co}_3\text{O}_4$  on  $\text{Al}_2\text{O}_3$  and  $\text{Al}_2(\text{SO}_4)_3$ , which yields  $\text{Co}_3\text{O}_4$  crystallites below the detection limit for XRD.

For the CoAlS2.5 sample an intense band split into three components at 16,100, 17,400 and 18,500  $\text{cm}^{-1}$  was observed. This corresponded to the transition  ${}^4\text{A}_2(\text{F}) \rightarrow {}^4\text{T}_1(\text{P})$ , assigned to tetrahedral  $\text{Co}^{2+}$  dispersed over the support carrier [19]. The spectra of the CoAl, CoAlS1.0, CoAlS1.8 and CoAlS3.2 samples exhibited distinctly different spectral features. According to the XRD data, the presence of the cobalt oxide  $\text{Co}_3\text{O}_4$  mixed valence spinel structure was evident for CoAl. The similarity of the bands of the CoAlS1.0, CoAlS1.8 and CoAlS3.2 samples leads to the conclusion that all these samples contain a mixture of tetrahedral  $\text{Co}^{2+}$  sites and the  $\text{Co}_3\text{O}_4$  phase. UV-vis-NIR spectra of this compound [20] exhibited bands corresponding to a mixture of tetrahedral  $\text{Co}^{2+}$  and octahedral  $\text{Co}^{3+}$  sites, with bands present at 13,900–15,000, 25,000 and 28,500–30,000  $\text{cm}^{-1}$ . However, in our work a significant band was also found around 24,000  $\text{cm}^{-1}$  in all the samples except for CoAlS2.5.

Cobalt oxide and many mixed oxides of  $\text{Co}^{2+}$ , including  $\text{CoAl}_2\text{O}_4$ , exhibit an absorption in the 25–27,000  $\text{cm}^{-1}$  region [19]. However,

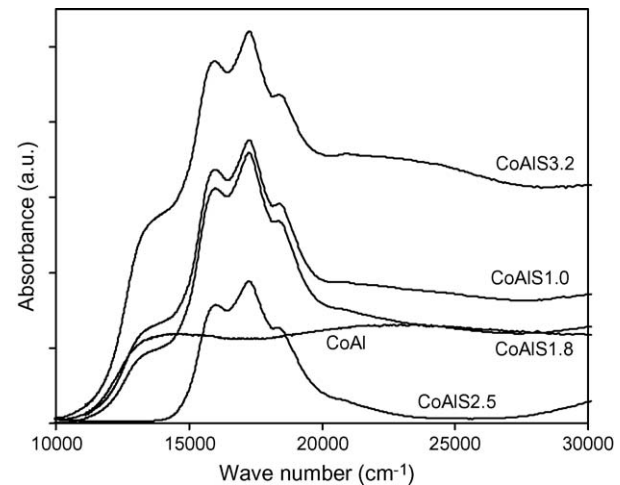


Fig. 5. UV-vis-NIR spectra obtained for the  $\text{CoO}_x/\text{Al}_2\text{O}_3\text{-SO}_4$  catalysts.

this band can in principle also be associated to octahedrally coordinated  $\text{Co}^{2+}$  [20]. In any case, the UV-vis-NIR spectroscopic results showed that sulphidation stabilised tetrahedral  $\text{Co}^{2+}$  at the expense of the  $\text{Co}_3\text{O}_4$  spinel phase. This explained why formation of  $\text{Co}_3\text{O}_4$ , known to aid direct  $\text{CH}_4$  combustion, was responsible for the reduced selectivity for the CoAl, CoAlS1.0, CoAlS1.8 and CoAlS3.2 catalyst samples.

As all the samples had been previously heat treated at 500 °C the thermograms presented in Fig. 6a are normalised to show the percentage weight losses from the samples when heated above this temperature, while in Fig. 6b the corresponding DTGA curves are given. Yang et al. [21] compared DTGA with conventional acidity measurements (FT-IR with pyridine, TPD with  $\text{NH}_3$ ) and found that it was a useful technique for characterising sulphate species on sulphated alumina. The results on our samples show that sulphidation of alumina not only increased the surface acidity but also induced changes to the acid centres, where three distinct types of surface sulphate could be detected: Brønsted type multi-layer precipitated sulphate, a crystalline neutral compound ( $\text{Al}_2(\text{SO}_4)_3$ ) and a strongly bound surface sulphate (super acidic Lewis centres) [22].

It was clearly seen that the weight losses from decomposition of sulphate species increased with increasing concentration of the  $\text{H}_2\text{SO}_4$  pretreatment solution. Furthermore, the type of sulphate species present on the catalysts seemed to depend on the acid concentration. At around 630 °C the peak originating from the

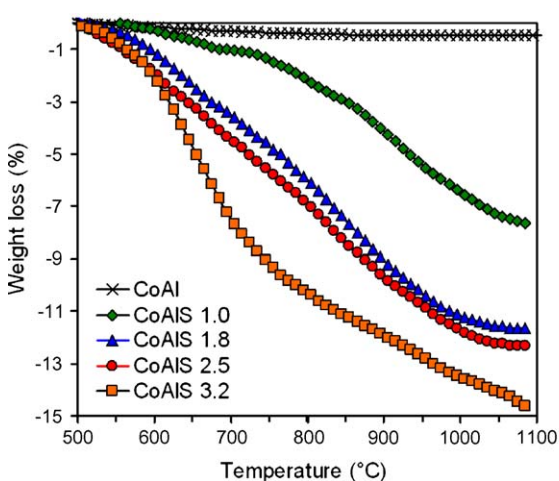
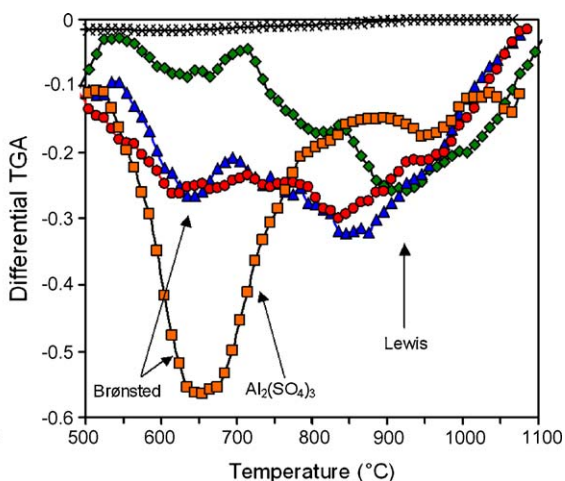
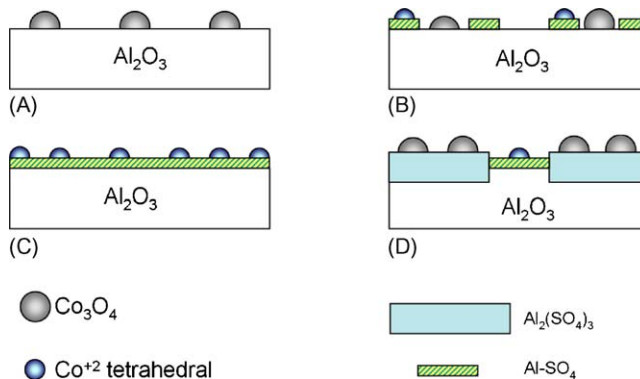


Fig. 6. Thermal gravimetric analyses for  $\text{CoO}_x/\gamma\text{-Al}_2\text{O}_3\text{-SO}_4$  supports.





**Fig. 7.** Suggested principal phases present on the surface of the catalysts, depending on the sulphuric acid concentration of the impregnating solution. (A) CoAl, (B) CoAlS<2.5, (C) CoAlS2.5 and (D) CoAlS3.2.

most abundant multi-layer sulphate was observed. The peak at around 700–750 °C, assigned to  $\text{Al}_2(\text{SO}_4)_3$ , increased considerably for the CoAlS3.2 catalyst, while the peak from the strongly bound Lewis acid sites that appears at temperatures higher than 900 °C was observed for all the catalysts.

Since all the catalysts have similar cobalt contents (approx. 3 %wt), these results indicated that the increase in the  $\text{SO}_4^{2-}$ -content provided a higher number of centres for anchorage of the SCR active Co (II)-sites, thus avoiding the formation of the unwanted  $\text{Co}_3\text{O}_4$  spinel up to a sulphur content of 5.0 %wt (2.5 M  $\text{H}_2\text{SO}_4$ ). From this point the formation of a new compound,  $\text{Al}_2(\text{SO}_4)_3$ , commenced that inhibited formation of the SCR-active centres and instead formation of non-selective  $\text{Co}_3\text{O}_4$  was observed. As a rough estimate of the area covered by a sulphate molecule, the classic equation  $a_m = 1.091(M_{\text{H}_2\text{SO}_4}/(\rho_{\text{H}_2\text{SO}_4} N_A))^{2/3}$  can be used [23]. With surface areas of around 200  $\text{m}^2/\text{g}$ , a sulphur content of 4.4% wt would correspond to a formal monolayer (using room temperature density for  $\text{H}_2\text{SO}_4$ ). Taking this value as a tentative guide, and assuming from the TGA data, that decomposition of sulphate species yields either  $\text{SO}_3$  or  $\text{SO}_2$  and  $1/2\text{O}_2$  [24] the behaviour of the sulphated catalysts can be explained in a straight forward manner. Fig. 7 shows the principal build up of the cobalt species on the surface of the alumina carrier with the sulphur concentration. When using sulphuric acid concentrations up to 2.5 M some alumina surface sites are still available for direct cobalt anchorage. Therefore, until a complete sulphate monolayer is reached, some  $\text{Co}_3\text{O}_4$  crystallites could be formed and thus the resulting catalysts will exhibit relatively poor selectivity, and burn  $\text{CH}_4$  readily with oxygen (Fig. 7a and b). When a complete sulphate monolayer is formed, but before excessive  $\text{Al}_2(\text{SO}_4)_3$  formation begins, the cobalt may only anchor to sulphate species, and thus the active tetrahedral  $\text{Co}^{2+}$  phase is formed (Fig. 7c). The results suggest that the 2.5 M impregnation solution provides the amount of sulphur needed to form a sulphate monolayer. At higher concentrations of sulphuric acid in the impregnation solution, the alumina solubility increases and therefore the non-active cobalt phases and  $\text{Al}_2(\text{SO}_4)_3$  are also formed (Fig. 7d). This hypothesis is in accordance with the increased pore volume observed for the CoAlS3.2 sample, since some of the formed  $\text{Al}_2(\text{SO}_4)_3$  will diffuse into the impregnation solution. It also further complements our interpretations of the UV-vis-, PZC-, TGA-data mentioned above.

#### 4. Conclusions

From our characterisation of the effect of the  $\text{H}_2\text{SO}_4$  concentration of the sulphate impregnation solution on  $\text{CoO}_x/\gamma\text{-Al}_2\text{O}_3\text{-SO}_4$

based DeNO<sub>x</sub> catalysts, it was shown that the active phase of these systems was related to tetrahedral Co(II)-SO<sub>4</sub> centres. The behaviour of these systems was controlled by the competition between the oxidation of  $\text{CH}_4$  by either oxygen or NO. The extension of both reactions depends on the concentration of the acid in the sulphidation step and the subsequent formation of different surface cobalt species. Thus, when the cobalt content in the catalyst is around 3.0 wt%, the optimal concentration both in terms of activity (high NO<sub>x</sub> conversion) and selectivity (low  $\text{CH}_4$  combustion) were obtained with sulphated samples containing 5% elemental sulphur, which in our case were obtained by using a  $\text{H}_2\text{SO}_4$  concentration of 2.5 M in the impregnation solution. At these conditions a maximum catalyst activity was observed and only tetrahedral Co(II)-SO<sub>4</sub> was detected. It was clear that there existed an ideal relationship between cobalt and sulphate in these systems, which could be changed either positively or negatively when the cobalt loading or sulphidation steps were modified.

When the sulphur was lower than 5%, higher ratios of crystalline  $\text{Co}_3\text{O}_4$  were detected, probably because of cobalt anchoring on available un-sulphated alumina surface. This enhanced the unwanted direct combustion of  $\text{CH}_4$  with  $\text{O}_2$ . The NO conversion capacity at high temperature was inversely related to the  $\text{CH}_4$  combustion with oxygen. Sulphated samples with sulphur contents higher than 5% suffered from deterioration of the chemical stability of the support, and subsequent unwanted synthesis of crystalline  $\text{Al}_2(\text{SO}_4)_3$  on the surface. The addition of cobalt in this support produces a high proportion of the unwanted  $\text{Co}_3\text{O}_4$  spinel.

#### Acknowledgments

The authors thank the Spanish Science and Innovation Ministry (Project CTTM2008-06876-C02-02/TECNO), the Comunidad de Madrid (CAM) (Program S0505/AMB/0406) and the CSIC-USACH collaboration project agreement 2008CL0017 for financial support. SBR thanks PSO (Project FU5201) for support.

#### References

- [1] M.D. Amiridis, T. Zhang, R.J. Farrauto, *Appl. Catal. B* 10 (1996) 203.
- [2] M. Shelef, *Chem. Rev.* 95 (1995) 209.
- [3] M.D. Fokema, J.Y. Ying, *Catal. Rev.* 43 (2001) 1.
- [4] V.I. Parvulescu, P. Grange, B. Delmon, *Catal. Today* 46 (1998) 233.
- [5] A.Z. Ma, M. Muhler, W. Grunert, *Appl. Catal. B* 27 (2000) 37.
- [6] R. Burch, J.P. Breen, C.J. Hill, B. Krutzsch, B. Konrad, E. Jobson, L. Cider, K. Eranen, F. Klingstedt, L.E. Lindfors, *Top. Catal.* 30–31 (2004) 19.
- [7] R. Burch, J.P. Breen, F.C. Meunier, *Appl. Catal. B* 39 (2002) 283.
- [8] J.L. d'Itri, W.M.H. Sachtler, *Catal. Lett.* 15 (1992) 289.
- [9] Y. Li, J.N. Armor, *Appl. Catal. B* 1 (1992) L31.
- [10] Y. Li, J.N. Armor, *Appl. Catal. B* 3 (1993) 55.
- [11] H. Hamada, *Catal. Today* 22 (1994) 21.
- [12] Y. Kintaichi, H. Hamada, M. Tabata, M. Sasaki, T. Ito, *Catal. Lett.* 6 (1990) 239.
- [13] T. Montanari, O. Marie, M. Daturi, G. Busca, *Appl. Catal. B* 71 (2007) 216.
- [14] V. Indovina, M.C. Campa, D. Pietrogiamomi, *J. Phys. Chem. C* 112 (2008) 5093.
- [15] K. Hadjivianov, B. Tsyntsarski, Tz. Venkov, D. Klissurski, M. Daturi, J. Saussey, J.-C. Lavalle, *Phys. Chem. Chem. Phys.* 5 (2003) 1695.
- [16] T. Maunula, J. Ahola, H. Hamada, *Appl. Catal. B* 26 (2000) 173.
- [17] J.C. Martín, P. Avila, S. Suárez, M. Yates, A.B. Martín-Rojo, C. Barthelemy, J.A. Martín, *Appl. Catal. B* 67 (2006) 270.
- [18] J.C. Martín, P. Avila, R. Fehrmann, S.B. Rasmussen, Book of Abstracts of 6th European Congress on Chemical Engineering, September 2007, Copenhagen-Denmark.
- [19] A.A. Verberckmoes, B.M. Weckhuysen, R.A. Schoonheydt, *Micropor. Mesopor. Mater.* 22 (1998) 165.
- [20] E. Finocchio, T. Montanari, C. Resini, G. Busca, *J. Mol. Catal. A: Chem.* 204 (2003) 535.
- [21] T.-s. Yang, T.-h. Chang, Ch.-t. Yeh, *J. Mol. Catal. A: Chem.* 115 (1997) 339–346.
- [22] J.C. Martín, S. Suárez Gil, M. Yates, P. Ávila, *Chem. Eng. J.* 150 (2009) 8–14.
- [23] J. Rouquerol, F. Rouquerol, C. Peres, Y. Grillet, M. Boudellal, in: S.J. Gregg, K.S.W. Sing, H.F. Stoeckli (Eds.), *Characterisation of Porous Solids*, Soc. Chem. Ind., London, 1979, p. 107.
- [24] T.-H. Kim, G.-T. Gong, B.G. Lee, K.-Y. Lee, H.-Y. Jeon, C.-H. Shin, H. Kim, K.-D. Jung, *Appl. Catal. A: Gen.* 305 (2006) 39.